Fano effect of a laterally coupled vertical triple quantum dot system*

He Ze-Long(贺泽龙)[a)b)], Lü Tian-Quan(吕天全)[a)†], and Zhang Di(张 迪)[c)]

[a)] Center for Condensed-Matter Science and Technology, Harbin Institute of Technology, Harbin 150080, China
[b)] Department of Electronic Engineering, Heilongjiang Institute of Technology, Harbin 150050, China
[c)] School of Physics and Electronic Engineering, Harbin Normal University, Harbin 150025, China

(Received 18 April 2012; revised manuscript received 5 September 2012)

Using the nonequilibrium Green's function technique, electron transport through a laterally coupled vertical triple quantum dot is investigated. The conductance as a function of electron energy is numerically calculated. The evolution of the conductance strongly depends on the configuration of dot levels and interdot coupling strengths.

Keywords: nonequilibrium Green's function, Fano effect, quantum dot, electron transport

PACS: 73.63.–b, 73.23.–b, 05.60.Gg **DOI:** 10.1088/1674-1056/22/2/027306

1. Introduction

In the past two decades, electron transport through a coupled quantum dot system has received much attention.[1–9] Coupled quantum dots enables one to investigate various important transport phenomena, such as quantum interference,[10,11] Kondo effects,[12–14] and the Fano effect[15–21] for its tunable parameters. Much attention has been paid to the Fano effect,[15–21] which arises from the interference between the resonant process and non-resonant process. Coupled multiple quantum dots can provide multiple channels for electronic coherent tunneling. Quantum interference of electron waves following along different paths can cause the Fano effect, which is a good probe of phase coherence in mesoscopic devices and shows a typical asymmetric line shape in the conductance spectrum. Experimentally, the Fano effect has been observed in quantum dots.[19–21]

The double quantum dot system has been designed for the quantum information applications, the fundamental studies of quantum molecular effects, and the exploitation of nanospintronic functionalities, and some new interference effects have been found.[22–27] A triple quantum dot device can be expected to lead to more interesting physics and applications. Three-dot structures have also received some attention.[28–32] For example, de Guevara and Orellana[28] proposed a parallel-coupled triple quantum dot molecule and investigated the Fano resonances and bound states in continuum. Li[32] investigated Fano resonance and flux-dependent transport through a triple-arm Aharonov–Bohm interferometer under an applied electric field. Though transport through a triple quantum dot molecule attached in parallel to leads has been investigated, the transport through a laterally coupled vertical triple quantum dot ring connected synchronously to two leads is less studied. In the present work, we do not take into consideration the interdot and intradot electron–electron interactions. This allows us to gain a much clearer physical insight into the dependences of the conductance of the system on the interdot couplings and dot levels. Our formalism is based on the nonequilibrium Green's function proposed by Jauho *et al.*[33] Though the model we considered is simple, some novel and interesting results are obtained arising from the coupling between the specific configuration of dot levels and interdot.

The remainder of the present article is organized as follows. Section 2 is devoted to a model Hamiltonian and the formula of the conductance. Numerical results and analysis are given in Section 3. The main conclusions are drawn in Section 4.

2. Model

We consider three single-level quantum dots forming a laterally coupled vertical triple quantum dot ring connected synchronously to two leads as shown in Fig. 1.

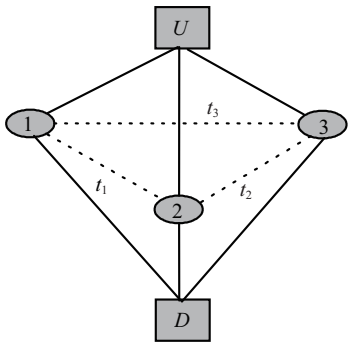


Fig. 1. Schematic setup of laterally coupled vertical triple quantum dot system.

*Project supported by the Youth Foundation of Heilongjiang Province, China (Grant No. QC2009C41) and the Heilongjiang Provincial Natural Science Foundation, China (Grant No. F200939).

†Corresponding author. E-mail: ltq@hit.edu.cn

© 2013 Chinese Physical Society and IOP Publishing Ltd

The full system can be described by the following Hamiltonian

$$H_{\rm total} = H_{\rm lead} + H_{\rm dots} + H_{\rm T}, \tag{1}$$

where the first term on the right-hand side, $H_{\rm lead}$, describes the leads in the noninteracting quasiparticle approximation,

$$H_{\rm lead} = \sum_{k,\sigma}\sum_{\alpha=U,D} \varepsilon_{k\alpha} C^{\dagger}_{k\alpha\sigma} C_{k\alpha\sigma} \tag{2}$$

with $C^{\dagger}_{k\alpha}$ ($C_{k\alpha}$) being the creation (annihilation) operator of the electron in lead α, and $\varepsilon_{k\alpha}$ denoting the corresponding single particle energy.

The second term of the Hamiltonian describes the triple quantum dot system

$$\begin{aligned} H_{\rm dots} =& \sum_{i\sigma} \varepsilon_{i\sigma} d^{\dagger}_{i\sigma} d_{i\sigma} - (t_1 d^{\dagger}_{1\sigma} d_{2\sigma} + t_2 d^{\dagger}_{2\sigma} d_{3\sigma} \\ &+ t_3 d^{\dagger}_{1\sigma} d_{3\sigma} + {\rm H.C.}), \end{aligned} \tag{3}$$

where $d^{\dagger}_i$ (d_i) ($i = 1,2,3$) represents the creation (annihilation) operator with the energy level $\varepsilon_{i\sigma}$ in the i-th quantum dot, and t_1 (t_2,t_3) is the tunneling coupling between the first (second, third) and the second (third, first) dots.

The last term on the right-hand side in Eq. (1), $H_{\rm T}$, describes the electron tunneling between dots and leads, and takes the form

$$H_{\rm T} = \sum_{i}\sum_{k\sigma}\sum_{\alpha=U,D} (t_{\alpha i\sigma} C^{\dagger}_{k\alpha\sigma} d_{i\sigma} + {\rm H.C.}), \tag{4}$$

where $t_{\alpha i\sigma}$ describes the dot–lead tunneling coupling, which is assumed to be independent of k. For simplicity, $t_{\alpha i\sigma} = |t_{\alpha i}|$, we define the line-width matrix elements as $\Gamma^{\alpha}_{ij\sigma} = 2\pi \sum_k t_{\alpha i\sigma} t^{*}_{\alpha j\sigma} \delta(\varepsilon - \varepsilon_{k\alpha})$, and then the matrix Γ^{α}_{σ} can be written as

$$\Gamma^{U(D)}_{\sigma} = \begin{pmatrix} \Gamma^{U(D)}_1 & \sqrt{\Gamma^{U(D)}_1 \Gamma^{U(D)}_2} & \sqrt{\Gamma^{U(D)}_1 \Gamma^{U(D)}_3} \\ \sqrt{\Gamma^{U(D)}_1 \Gamma^{U(D)}_2} & \Gamma^{U(D)}_2 & \sqrt{\Gamma^{U(D)}_2 \Gamma^{U(D)}_3} \\ \sqrt{\Gamma^{U(D)}_1 \Gamma^{U(D)}_3} & \sqrt{\Gamma^{U(D)}_2 \Gamma^{U(D)}_3} & \Gamma^{U(D)}_3 \end{pmatrix}, \tag{5}$$

where Γ^{α}_i is Γ^{α}_{ii} ($i = 1,2,3$) for short.

To describe the non-equilibrium states in the system, we introduce the retarded, advanced, and 'lesser' Green's functions as follows:

$$G^{\rm r}_{AB}(t,t') = \langle\langle A(t), B(t')\rangle\rangle^{\rm r} = -{\rm i}\theta(t-t')\langle [A(t), B(t')]_+\rangle, \tag{6}$$

$$G^{\rm a}_{AB}(t,t') = \langle\langle A(t), B(t')\rangle\rangle^{\rm a} = {\rm i}\theta(t'-t)\langle [A(t), B(t')]_+\rangle, \tag{7}$$

$$G^{<}_{AB}(t,t') = \langle\langle A(t), B(t')\rangle\rangle^{<} = {\rm i}\langle B(t')A(t)\rangle. \tag{8}$$

Our calculations are limited to the steady state where the Green's functions depend only on the variable $\Delta t = t - t'$. By Fourier transforming with respect to variable $t - t'$ in $\langle\langle A(t-t'), B(0)\rangle\rangle$, we can obtain $\langle\langle A, B\rangle\rangle_{\omega}$. In the present investigation, the knowledge of the Green's functions $\langle\langle d_i, d^{\dagger}_i\rangle\rangle_{\omega}$ ($i = 1,2,3$) enables us to determine all the transport characteristics of the system. In order to calculate them, we use both the Dyson equation and the equation of motion for each Green's function. The retarded (advanced) Green's function can be written as

$$G^{\rm r}_{\sigma}(\varepsilon) = (G^{\rm a}_{\sigma}(\varepsilon))^{\dagger} = \begin{pmatrix} \varepsilon - \varepsilon_{1\sigma} + \frac{\rm i}{2}(\Gamma^{U}_{11\sigma} + \Gamma^{D}_{11\sigma}) & t_1 + + \frac{\rm i}{2}(\Gamma^{U}_{12\sigma} + \Gamma^{D}_{12\sigma}) & t_3 + \frac{\rm i}{2}(\Gamma^{U}_{13\sigma} + \Gamma^{D}_{13\sigma}) \\ t_1 + \frac{\rm i}{2}(\Gamma^{U}_{21\sigma} + \Gamma^{D}_{21\sigma}) & \varepsilon - \varepsilon_{2\sigma} + \frac{\rm i}{2}(\Gamma^{U}_{22\sigma} + \Gamma^{D}_{22\sigma}) & t_2 + + \frac{\rm i}{2}(\Gamma^{U}_{23\sigma} + \Gamma^{D}_{23\sigma}) \\ t_3 + \frac{\rm i}{2}(\Gamma^{U}_{31\sigma} + \Gamma^{D}_{31\sigma}) & t_2 + + \frac{\rm i}{2}(\Gamma^{U}_{32\sigma} + \Gamma^{D}_{32\sigma}) & \varepsilon - \varepsilon_{3\sigma} + \frac{\rm i}{2}(\Gamma^{U}_{33\sigma} + \Gamma^{D}_{33\sigma}) \end{pmatrix}^{-1}. \tag{9}$$

The conductance at zero temperature reads

$$G_{\sigma}(\varepsilon_F) = \frac{e^2}{\hbar} {\rm Tr}\left[G^{\rm a}_{\sigma}(\varepsilon)\Gamma^{D}_{\sigma} G^{\rm r}_{\sigma}(\varepsilon)\Gamma^{U}_{\sigma}\right]\Big|_{\varepsilon=\varepsilon_{\rm F}}, \tag{10}$$

where $\varepsilon_{\rm F}$ is the Fermi level.

3. Numerical results

Using the formulae obtained above, one can numerically calculate the basic transport characteristics of the system. In the following numerical analysis, we presume that $\Gamma^{\alpha}_1 = \Gamma^{\alpha}_2 = \Gamma^{\alpha}_3 = \Gamma(\alpha \in U, D)$, and take Γ as the energy unit.

The interdot coupling can be tuned by adjusting the height and thickness of the tunneling barrier between two dots through gate voltage. We first study the linear transport properties in the case of symmetrical interdot tunneling couplings, i.e., $t_1 = t_2 = t_3 = t$. Figure 2 presents the conductance with respect to the electron energy with $\varepsilon^0_i = 0$ ($i = 1,2,3$) for three different values of t. As $t = 0$ (see the solid-line in Fig. 2), the conductance spectrum shows only one resonance peak located at the energy level of the quantum dot, i.e., $\varepsilon^0_i = 0$. These three quantum dots can be seen as isolated atoms and the conductance peak is the atomic spectrum of a single quantum dot. When $t \neq 0$ (see the dashed line and the dotted line in Fig. 2), the conductance spectrum still gives one resonance peak located at $\varepsilon^0_i + 2t$. These three quantum dots form an "artificial molecule", and the resonances are spectra of molecular levels. However, our model is completely symmetrical in space, and quantum dots 1, 2, and 3 are completely equivalent, which leads to the degeneracy of three molecular states. This also means that the degeneracy of energy is not lifted by varying

the aligned interdot tunneling coupling strength.

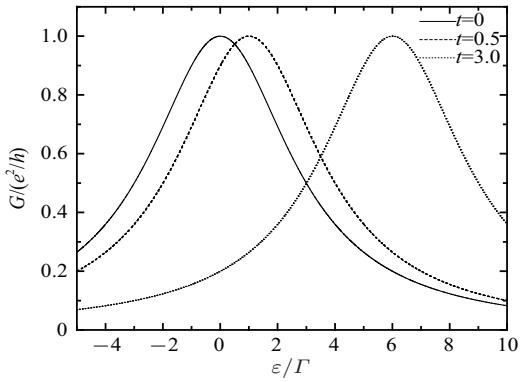


Fig. 2. Conductances versus electron energy for three different values of t with parameters being $\varepsilon^0_{1(2,3)} = 0$.

Figures 3 and 4 display the cases of mismatched levels, showing the interesting conductance spectra. Figure 3 indicates the case of $\varepsilon^0_1 = -1$ and $\varepsilon^0_{2,3} = 0$ for three different interdot tunneling coupling strengths. In this case, the partially degenerate energy levels still occur because of the equivalence between the second dot and third dot. So each conductance spectrum displays two peaks. If $t = 0$, the three quantum dots can be seen as isolated atoms. As shown by the solid line in Fig. 3, two resonance peaks are located at two atomic energy levels: $\varepsilon = -1$ and $\varepsilon = 0$, respectively, and a conductance dip between two resonance peaks is found. The right peak is wider than the left one. When considering the tunneling coupling between the quantum dots, the three quantum dots couple as a molecule. The resonant levels through the molecule are renormalized, and some interesting results can be found and shown by the dashed and dotted lines in Fig. 3. With the increase of interdot tunneling coupling strength, one can clearly observe that the right peak moves rightwards and its width widens, while the left peak moves leftwards and develops into Fano antiresonance with narrow width. At the same time, the conductance dip evolves into a Fano dip. It should be pointed out that the dashed line in the conductance spectrum is very similar to the case of double quantum dots connected in parallel configuration (see Ref. [34]).

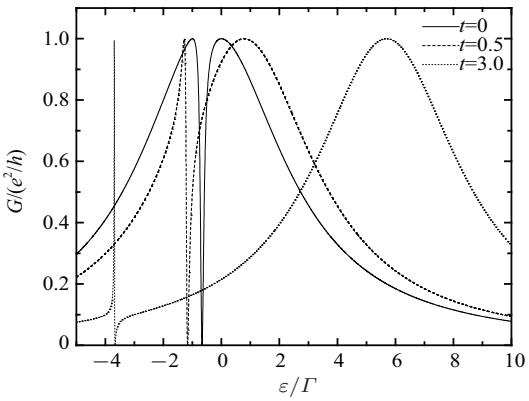


Fig. 3. Conductances versus electron energy for several different values of t with parameters being $\varepsilon^0_1 = -1$ and $\varepsilon^0_{2,3} = 0$.

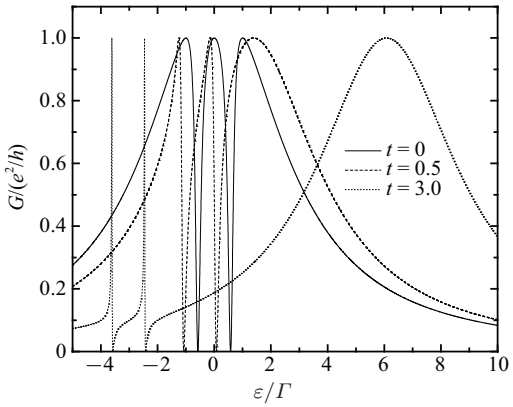


Fig. 4. Conductances versus electron energy for three different values of t with parameters being $\varepsilon^0_1 = -1$, $\varepsilon^0_2 = 0$, and $\varepsilon^0_3 = 1$.

Figure 4 shows the curves in the case of $\varepsilon^0_1 = -1$, $\varepsilon^0_2 = 0$, and $\varepsilon^0_3 = 1$. In this case, all the quantum dots are not equivalent, which can lead to complete splitting of the degenerate energy level. As expected, each conductance spectrum displays three peaks related to three states. When $t = 0$, three resonance peaks occur at the energy level of isolated atoms, respectively, i.e., $\varepsilon = -1, 0, +1$. Moreover, three peaks keep mirror symmetry with respect to energy level $\varepsilon = 0$. When $t = 0.5$, the width of the peak located at $\varepsilon = 1$ widens, however, the widths of two peaks located at $\varepsilon = -1, 0$ become narrow. If t is large enough, i.e., $t = 3$, the two left resonance peaks evolve into two typical Fano antiresonance peaks and their line-shapes are similar. It can be seen from the above analysis that for quantum dots with different energies, three molecular states always contribute to the conductance.

Figure 5 depicts the conductances each as a function of the electron energy level for the different configurations of interdot tunneling coupling strengths. When the interdot tunneling coupling strengths of three quantum dots take the same values as shown by the solid line in Fig. 5, only one resonance peak appears at $\varepsilon^0_i + 2t$, which is the same result as the above discussion indicates. For $t_1 = t_2 \neq t_3$, as shown by the dashed line in Fig. 5, one resonance peak and one Fano peak appear in the conductance spectrum. Compared with the

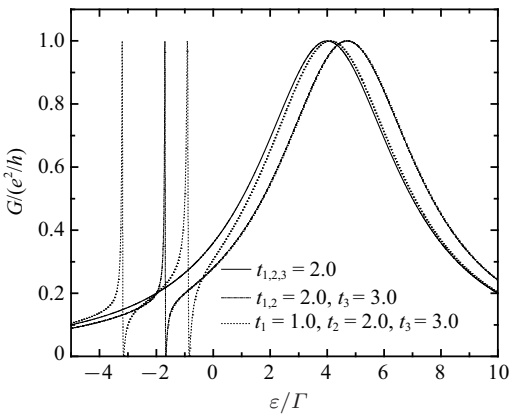


Fig. 5. Conductances versus electron energy for the different configurations of interdot couplings with parameters being $\varepsilon^0_{1(2,3)} = 0$.

case of $t_{1(2,3)} = 2.0$, the resonance peak moves rightwards. If $t_1 \neq t_2 \neq t_3$, as shown by the dotted line in Fig. 5, one resonance peak and two Fano peaks in the conductance spectrum can be found. Here, the Fano effect results from the quantum interference of electron waves following different paths. According to the above discussion, we can determine the configuration of interdot tunneling couplings by observing the conductance spectrum.

4. Conclusions

We investigated the quantum transport through a laterally coupled vertical triple quantum dot ring under DC bias voltage. The conductance $G(\varepsilon)$ as a function of electron energy ε is analyzed. Some significant results are obtained as follows: (i) as one takes symmetrical interdot tunneling couplings and mismatched levels, the Fano resonance peaks occur in the conductance spectrum and the conductance dip evolves into the Fano dip with the increase of interdot tunneling couplings; (ii) as one takes the different configurations of interdot tunneling coupling strengths and aligned levels, the quantum interference of electron waves following different paths leads to the Fano effect.

References

[1] Huang R, Wu S Q and Yan C H 2010 *Chin. Phys.* B **19** 077302
[2] Zhao H K 1997 *Phys. Lett.* A **226** 105
[3] Xie Y, Duan S Q, Chu W D and Yang N 2011 *Chin. Phys.* B **19** 117302
[4] Wen R, Zhang D P and Tian G S 2012 *Chin. Phys.* B **21** 037401
[5] He Z L, Lü T Q, Li H and Yin H T 2006 *Phys. Lett.* A **360** 199
[6] He Z L and Lü T Q 2012 *Phys. Lett.* A **376** 2501
[7] Lü H F and Guo Y 2007 *Phys. Rev.* B **76** 045120
[8] Gong W J, Zheng Y S, Liu Y, Kariuki F N and Lü T Q 2008 *Phys. Lett.* A **372** 2934
[9] An X T and Liu J J 2008 *Phys. Lett.* A **372** 6790
[10] Donarini A, Begemann G and Grifoni M 2010 *Phys. Rev.* B **82** 125451
[11] Hatef A and Singh M R 2010 *Phys. Rev.* A **81** 063816
[12] Malecki J and Affleck I 2010 *Phys. Rev.* B **82** 165426
[13] Sun Q and Guo H 2001 *Phys. Rev.* B **64** 153306
[14] Žitko R 2010 *Phys. Rev.* B **81** 115316
[15] Fano U 1961 *Phys. Rev.* **124** 1866
[16] Sun Q, Wang J and Guo H 2005 *Phys. Rev.* B **71** 165310
[17] Lu H, Lü R and Zhu B 2006 *Physica* E **34** 538
[18] Chi F and Zheng J 2008 *Appl. Phys. Lett.* **92** 062106
[19] Kobayashi K, Aikawa H, Katsumoto S and Iye Y 2002 *Phys. Rev. Lett.* **88** 256806
[20] Zacharia I G, Goldhaber-Gordon D, Granger G, Kastner M A and Khavin Y B 2001 *Phys. Rev.* B **64** 155311
[21] Göres J, Goldhaber-Gordon D, Heemeyer S and Kastner M A 2000 *Phys. Rev.* B **62** 2188
[22] Yanaka Y and Kawakami N 2005 *Phys. Rev.* B **72** 085304
[23] Kubala B and Konig J 2002 *Phys. Rev.* B **65** 245301
[24] Ding G H, Kim C K and Nahm K 2005 *Phys. Rev.* B **71** 205313
[25] Lu H, Lü R and Zhu B 2005 *Phys. Rev.* B **71** 235320
[26] Peng J, Wang B and Xing D Y 2005 *Phys. Rev.* B **71** 214523
[27] Kang K and Cho S Y 2004 *J. Phys.*: *Condens. Matter* **16** 117
[28] de Guevara M L L and Orellana P A 2006 *Phys. Rev.* B **73** 205303
[29] Chen K and Chang C 2008 *J. Appl. Phys.* **103** 07B708
[30] He Z L, Lü T Q, Cui L, Xue H J, Li L J and Yin H T 2011 *Chin. Phys.* B **20** 117303
[31] He Z L, Lü T Q, Li H, Li L J, Cui L and Xue H J 2011 *Phys. Scr.* **84** 035703
[32] Li Y 2007 *J. Phys.*: *Condens. Matter* **19** 496219
[33] Jauho A P, Wingreen N S and Meir Y 1994 *Phys. Rev.* B **50** 5528
[34] de Guevara M L L, Claro F and Orellana P A 2003 *Phys. Rev.* B **67** 195335